FAILURE ANALYSIS OF ANISOTROPIC PLATES BY THE BOUNDARY ELEMENT METHOD

A. Sahli* **S. Boufeldja** **S. Kebdani** **O. Rahmani**

Faculté de Génie Mécanique
Université des Sciences et de la Technologie d'Oran
Oran, Algérie

ABSTRACT

This paper presents a dynamic formulation of the boundary element method for stress and failure criterion analyses of anisotropic thin plates. The elastostatic fundamental solutions are used in the formulations and inertia terms are treated as body forces. The radial integration method (RIM) is used to obtain a boundary element formulationithout any domain integral for general anisotropic plate problems. In the RIM, the augmented thin plate spline is used as the approximation function. A formulation for transient analysis is implemented. The time integration is carried out using the Houbolt method. Integral equations for the second derivatives of deflection are developed and all derivatives of fundamental solutions are computed analytically. Only the boundary is discretized in the formulation. Numerical results show good agreement with results available in literature as well as finite element results.

Keywords: Boundary element method, Radial integration method, Plates, Composite materials, Dynamic of plates, Stress analyses and failure criterion.

1. INTRODUCTION

Rarely, damage caused by low velocity impact are detected with the naked eye. Since they cannot be found, the harm caused by low velocity impact in composite materials are considered potentially hazardous. In general, the cracking of the matrix and fiber breakage are the initial damage prior to delamination. The stiffness of the damaged material and therefore the structure can be significantly reduced by damage. This loss of stiffness may even cause a catastrophic failure. For these reasons, it is important to develop tools that enable analysis of structures of composite materials under low velocity impact.

The numerical analysis of damage caused by low velocity impact has been made mainly by the finite element method (FEM). Lakshminarayana and murthy, [1]; Luo *et al*. [2] made a dynamic analysis of a structure using a commercial program to predict damage to the material without regard to the progressive failure analysis aid. Zhao and Cho [3] analyzed the onset of damage in a composite material using 8 noded shell elements. Ganapathy and Rao [4] analyzed the damage in a laminated curved shell element using a double curvature of 48 degrees of freedom. Li *et al*. [5,6] presented a numerical model to simulate the process of low velocity impact based on a Mindlin plate element of 9 nodes. In literature review, were not found any articles in the literature where damage caused by low velocity impact was analyzed using the boundary element method (BEM). However, some characteristics of BEM makes it attractive for this analysis aid, for example, its high rate of convergence in the analysis of problems of high gradients, and the case of propagation of waves arising from the impact.

The boundary element formulations have been applied to problems of anisotropic plates in flexion, considering the Kirchhoff's theory, and theories of shear deformable plates. Shi and bezine [7] provide a boundary element analysis of plate bending problems using the fundamental solution proposed by Wu and altiero [8] based on the assumptions of flexion of the Kirchhoff plate. Rajamohan and Raamachandran [9] proposed a formulation in which the singularities are avoided by points sources placed outside the domain. Paiva *et al*. [10] presented an analytic treatment for singular integrals and hypersingular formulation proposed by Shi and bezine [7]. Shear deformable plates has been analyzed using the boundary element method by Wang and Schweizerhof [11,12], with the fundamental solution proposed by Wang and Schweizerhof [13].

In the boundary element method for plate bending, the presence of distributed force in the domain do appear in the integral equation. Aiming to solve these integrals, the integration scheme by cells can give accurate results, as shown by Shi and bezine [7] for problems of anisotropic plates in flexion. However, the domain discretization into cells reduces one of the main advantages of the boundary element method and the discretization that only the outline. Rajamohan and Raamachandran [9] have proposed the use of private

* Corresponding author (sahli_ah@yahoo.com)

DOI : 10.1017/jmech.2014.65
Copyright © 2014 The Society of Theoretical and Applied Mechanics, R.O.C.
https://doi.org/10.1017/jmech.2014.65 Published online by Cambridge University Press

solutions to approximate the domain discretization as an alternative to this procedure. However, the use of particular solutions requires finding a function satisfying the governing equation. Depen ding on how complex the ruler equation, this function can be difficult to find.

In this paper, domain integrals due to distributed loads are transformed into boundary integrals by radial integration method. This method was proposed by Gao [15] for three-dimensional elasticity isotropic problems and extended by Albuquerque *et al*. [16] to anisotropic Kirchhoff plate.

2. MECHANICAL FAILURES IN COMPOSITE MATERIALS

The theories of failure are central to the determination of criteria for the prediction of failure of a material against a bi-or three-dimensional state tensions. When the state of tensions is one-dimensional, the simple criterion to control the amount of tension so as not to exceed the yield stress or rupture of the material is sufficient to determine fault. However, a complex state of tensions requires own theories for the type of material.

The formulation developed in this paper is applied to compute the stress and displacements of plane structures of composite laminates subjected to transverse loads to the structure plane. Will be studied in this work the failure criteria for composite materials, focusing on the quadratic criterion of Tsai and Wu [17].

Looking at the data presented it follows easily that the failure in composite materials and more complex than in isotropic materials, it involves the analysis of a larger number of variables. Thus, the criteria traditionally used in the design of machines and structures in materials with isotropic behavior may not be appropriate and may even lead the designer to catastrophic errors if used wrongly.

The utilization of more complex criteria leads to more accurate results, but at a higher cost. The criteria of maximum stress and maximum deformation require the analysis of three different fault conditions for the determination of the actual limit. This inconvenient is eliminated with the development of quadratic criteria such as Tsai – Hill, Hill [18], Tsai [19], and Tsai - Wu [17]. While the first Tsai - Hill is simpler to use the second Tsai-Wu presents a better accuracy of the results. All these criteria however require a larger number of tests of composite materials (unidirectional laminate) than those required for determining the characteristics of an isotropic material.

3. BASIC RELATIONS FOR ANISOTROPIC PLATES

Consider a plate following the assumptions defined in the previous section. As shown by Lekhnitskii [20], the lateral mid-surface deflection w satisfies the differential equation:

$$D_{11}\frac{\partial^4 w}{\partial x^4}+4D_{16}\frac{\partial^4 w}{\partial x^3\partial y}+2(D_{12}+2D_{66})\frac{\partial^4 w}{\partial x^2\partial y^2}+4D_{26}\frac{\partial^4 w}{\partial x\partial y^3}+D_{22}\frac{\partial^4 w}{\partial y^4}=g \quad (1)$$

where the D_{ij} are the flexural rigidities of the anisotropic plate and g is the transverse load intensity.

The general solution for w in Eq. (1) depends on μ_1, μ_2, $\bar{\mu}_1$ and $\bar{\mu}_2$ the roots of the characteristic equation, given by

$$D_{22}\,\mu^4+4D_{26}\,\mu^3+2(D_{12}+2D_{66})\mu^2+4D_{16}\,\mu+D_{11}=0 \quad (2)$$

The roots of this equation are always complex for a homogeneous material. The complex roots $\mu_1 = d_1 + e_1 i$ and $\mu_2 = d_2 + e_2 i$ are known as the transverse-displacement complex parameters.

4. BOUNDARY INTEGRAL EQUATION FOR BENDING PROBLEMS OF ANISOTROPIC PLATES

As shown by Shi and Bezine [21], the equilibrium Eq. (1) can be transformed into a boundary integral equation given by

$$\begin{aligned} Kw(Q)+\int_\Gamma\left[V_n^*(Q,P)\,w(P)-m_n^*(Q,P)\frac{\partial w(P)}{\partial n}\right]d\Gamma(P) \\ +\sum_{i=1}^{N_c}R_{ci}^*(Q,P)\,w_{ci}(P)=\sum_{i=1}^{N_c}R_{ci}(P)w_{ci}^*(Q,P) \\ +\int_\Gamma\left[V_n(P)\,w^*(Q,P)-m_n(P)\frac{\partial w^*(Q,P)}{\partial n}\right]d\Gamma(P) \\ +\int_\Omega g(P)w^*(Q,P)\,d\Omega \end{aligned} \quad (3)$$

where $\partial(\ )/\partial n$ is the derivative in the direction of the outward vector n that is normal to the boundary Γ; m_n and V_n are, respectively, the normal bending moment and the Kirchhoff equivalent shear force on the boundary Γ; R_c is the thin-plate reaction of the corners; w_c is the transverse displacement of the corners; P is the field point; Q is the source point; and an asterisk denotes a fundamental solution.

The constant K is introduced in order to take account of the possibilities that the point Q can be placed in the domain, on the boundary, or outside the domain. If the point Q is on a smooth boundary, then $K = 1/2$.

In order to have an equal number of equations and unknown variables, it is necessary to write an integral equation corresponding to the derivative of the displacement $w(Q)$ with respect to a Cartesian coordinate system fixed to the source point. The axis directions of this coordinate system are coincident with the directions of two vectors that are normal and tangential to the boundary at the source point.

For the particular case where the source point Q is

https://doi.org/10.1017/jmech.2014.65 Published online by Cambridge University Press

placed on a smooth boundary, the boundary equation is given by Paiva, [22]:

$$\frac{1}{2}\frac{\partial w(Q)}{\partial n_1}+\int_\Gamma\left[\frac{\partial V^*}{\partial n_1}(Q,P)\,w(P)-\frac{\partial m_n^*(Q,P)}{\partial n_1}\frac{\partial w(P)}{\partial n}\right]d\Gamma(P)$$
$$+\sum_{i=1}^{N_c}\frac{\partial R_{ci}^*}{\partial n_1}(Q,P)w_{ci}(P)=\sum_{i=1}^{N_c}R_{ci}(P)\frac{\partial w_{ci}^*}{\partial n_1}(Q,P)$$
$$+\int_\Gamma\left[V_n(P)\frac{\partial w^*}{\partial n_1}(Q,P)-m_n(P)\frac{\partial}{\partial n_1}\left[\frac{\partial w^*(Q,P)}{\partial n}\right]\right]d\Gamma(P)$$
$$+\int_\Omega g(P)\frac{\partial w^*}{\partial n_1}(Q,P)\,d\Omega \tag{4}$$

where $\partial(\ )/\partial n_1$ is the derivative in the direction of the outward vector n1 normal to the boundary Γ at the source point Q.

It is important to say that it is possible to use only Eq. (3) in a boundary element formulation, by using the boundary nodes and an equal number of points external to the domain of the problem as source points.

Fundamental solutions for anisotropic thin plates can be found in Shi and Bezine [21] and Albuquerque *et al.* [16].

5. TRANSFORMATION OF DOMAIN INTEGRALS INTO BOUNDARY INTEGRALS FOR ANISOTROPIC PLATES IN FLEXION

An application of the boundary element method requires, preferably, that the fundamental solution to the problem in consideration is known. This fundamental solution should take into account all the terms of the governing equation to obtain a formulation where only the boundary is discretized. When this is not possible, the terms not considered in obtaining the fundamental solution will produce comprehensive domain which preferably should be transformed into boundary integrals. The first alternative is to do the exact transformation of the domain integral in boundary integral. However, this is only possible when the terms are considered not only functions of geometry (distributed load, for example). The second alternative is to transfer the effects of the domain integral to the contour using the method of boundary element dual reciprocity or the radial integration, Albuquerque and Aliabadi [23]. These procedures are more general and can be used for any terms. In this paper, the domain integral arising from the distributed load will be transformed into boundary integrals by exact transformation, while that the terms of inertia will be processed using the method of radial integration.

As can be seen in Eqs. (3) and (4), a couple of domain integrals in the formulation due to the distributed load domain and the terms of inertia. These integrals can be calculated by direct integration; using cells in the area Ωg (see Fig. 1). However, the boundary element formulation loses its main attraction, *i.e*, the only boundary discretization. Here, the integral domain arising from distributed loads are transformed into boundary integrals by an exact transformation.

Consider the plate of Fig. 1, under a load g, applied over an area Ωg. Assuming that the load g has a linear distribution $(Ax + By + C)$ in the area Ωg, the domain integral can be written as

$$\int_{\Omega_g} gw^*\,d\Omega=\int_{\Omega_g}(Ax+By+C)\,w^*\rho d\rho d\theta \tag{5}$$

or

$$\int_{\Omega_g} gw^*\,d\Omega=\int_{\theta}\int_{0}^{r}(Ax+By+C)\,w^*\rho d\rho d\theta \tag{6}$$

where r is the value of ρ at a point on the boundary Γ_g.

Defining $F*$ as the integral

$$F^*=\int_0^r(Ax+By+C)\,w^*\rho d\rho \tag{7}$$

we can write

$$\int_{\Omega_g} gw^*\,d\Omega=\int_\theta F^*\,d\theta \tag{8}$$

Considering an infinitesimal angle $d\theta$, the relation between the arc length $rd\theta$ and the infinitesimal boundary length $d\Gamma$ can be written as

$$\cos\alpha=\frac{rd\theta/2}{d\Gamma/2}\quad\text{or}\quad d\theta=\frac{\cos\alpha}{r}d\Gamma \tag{9}$$

where α is the angle between the unit vectors r and n.

Using the properties of the inner product of the unit vectors n and r, we can write

$$d\theta=\frac{n.r}{r}d\Gamma \tag{10}$$

Finally, by substituting Eq. (9) into Eq. (6), the domain integral in Eq. (3) can be written as a boundary integral given by

$$\int_{\Omega_g} gw^*\,d\Omega=\int_{\Gamma_g}\frac{F^*}{r}n.r\,d\Gamma \tag{11}$$

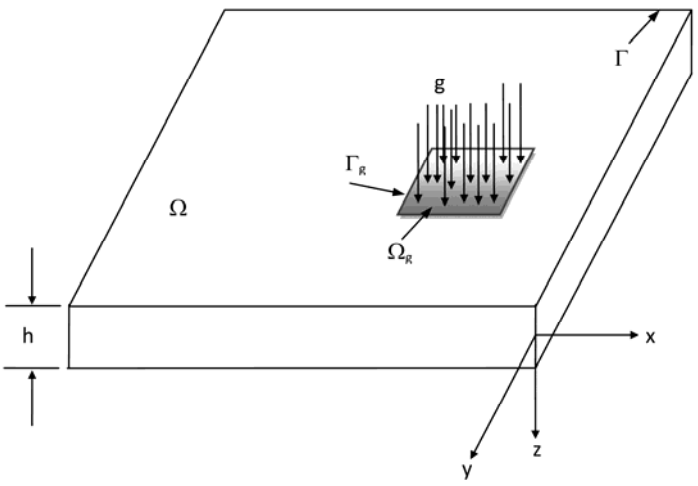


Fig. 1 Thin plate.

https://doi.org/10.1017/jmech.2014.65 Published online by Cambridge University Press

Provided that

$$x = \rho\cos\theta \quad \text{and} \quad y = \rho\sin\theta \tag{12}$$

the integral F^* can be written as

$$F^* = \int_0^r \frac{1}{8\pi}(A\rho\cos\theta + B\rho\sin\theta + C) \cdot\left[C_1R_1 + C_2R_2 + C_3(S_1 - S_2)\right]\rho d\rho \tag{13}$$

$$F^* = \frac{1}{8\pi}\left\{(A\cos\theta + B\sin\theta)\int_0^r \rho^2\left[C_1R_1 + C_2R_2 + C_3(S_1 - S_2)\right]d\rho + C\int_0^r \rho\left[C_1R_1 + C_2R_2 + C_3(S_1 - S_2)\right]d\rho\right\} \tag{14}$$

where

$$\rho = \left[(x - x_0)^2 + (y - y_0)^2\right]^{\frac{1}{2}}$$

x and y are the coordinates of the field point P, x_0 and y_0 are the coordinates of the source point Q,

$$\theta = \arctan\frac{y - y_0}{x - x_0},$$

$$C_1 = \frac{(d_1 - d_2)^2 - (e_1^2 - e_2^2)}{GHe_1},\quad C_2 = \frac{(d_1 - d_2)^2 + (e_1^2 - e_2^2)}{GHe_2},$$

$$C_3 = \frac{4(d_1 - d_2)}{GH},$$

$$G = (d_1 - d_2)^2 + (e_1 + e_2)^2,\quad H = (d_1 - d_2)^2 + (e_1 - e_2)^2$$

$$R_i = \rho^2\left[(\cos\theta + d_i\sin\theta)^2 - e_i^2\sin^2\theta\right] \times\left\{\ln\left[\frac{\rho^2}{a^2}\left((\cos\theta + d_i\sin\theta)^2 + e_i^2\sin^2\theta\right)\right] - 3\right\} - 4\rho^2 e_i\sin\theta(\cos\theta + d_i\sin\theta)\arctan\frac{e_i\sin\theta}{\cos\theta + d_i\sin\theta}$$

$$S_i = \rho^2 e_i\sin\theta(\cos\theta + d_i\sin\theta) \times\left\{\ln\left[\frac{\rho^2}{a^2}\left((\cos\theta + d_i\sin\theta)^2 + e_i^2\sin^2\theta\right)\right] - 3\right\} + \rho^2\left[(\cos\theta + d_i\sin\theta)^2 - e_i^2\sin^2\theta\right]\arctan\frac{e_i\sin\theta}{\cos\theta + d_i\sin\theta}$$

The repeated index i in the terms of R_i and S_i does not imply summation. The coefficient a is an arbitrary constant, taken as equal to 1.

di and ei are respectively the real and imaginary parts of the roots μ_i of the characteristic Eq. (2).

Following a procedure similar to that used to obtain Eq. (14), the domain term of Eq. (4) can be written as

$$\int_\Omega g(P)\frac{\partial w^*}{\partial n_1}(Q, P)\,d\Omega = \int_\theta \frac{G^*}{r}n.rd\Gamma \tag{15}$$

where

$$G^* = \int_0^r (Ax + By + C)\frac{\partial w^*}{\partial n_1}\rho d\rho = \frac{1}{8\pi}\left\{(A\cos\theta + B\sin\theta)\int_0^r \rho^2\left[C_1\frac{\partial R_1}{\partial n_1} + C_2\frac{\partial R_2}{\partial n_1} + C_3\left(\frac{\partial S_1}{\partial n_1} - \frac{\partial S_2}{\partial n_1}\right)\right]d\rho + C\int_0^r \rho\left[C_1\frac{\partial R_1}{\partial n_1} + C_2\frac{\partial R_2}{\partial n_1} + C_3\left(\frac{\partial S_1}{\partial n_1} - \frac{\partial S_2}{\partial n_1}\right)\right]d\rho\right\} \tag{16}$$

As can be seen, Eqs. (14) and (16) are not h-dependent. These integrals can be evaluated analytically.

Although in this work the loads on the domain are considered as uniformly or linearly distributed, the procedure presented in this section can be extended to other, higher-order loads.

6. TRANSIENT PROBLEMS

The boundary element method for radial integration is applied to calculate the displacement fields for transient problems in the time domain. The integration in time is performed using the method proposed by Houbolt [24] because it has already been shown by Loeffler and Mansur [25] that the Houbolt method is most appropriate to use the direct integration in time combined with the boundary element method for radial integration, and used by Albuquerque *et al*. [26]. An important feature of the Houbolt method is that it has a high numerical damping. This damping makes the results obtained by the boundary element integration of radial smoother than those obtained by other formulations of the boundary element method applied to elasto-dynamic Fedelinsk *et al*. [27] and Chirino *et al*. [28]. However, the numerical damping can be reduced using smaller time steps. Sometimes, to be able to reduce the time step and obtain a greater precision of results is necessary to refine the mesh or increasing the number of internal nodes.

Consider the unique body forces in a body of domain Ω and boundary Γ are due to the acceleration field $\ddot{w}$, *i.e.*:

$$b = \rho h\ddot{w} \tag{17}$$

The Houbolt scheme is framed between the methods of multiple steps, because it uses not only the values of the previous step to determine the current values, but three other steps in the past. To carry out the integration over a time period T, this period is divided into N equal intervals $\Delta\tau$ | $(T = N\Delta\tau)$. The acceleration in $\tau + \Delta\tau$ is approximated by the finite difference expression:

$$\ddot{w}_{\tau+\Delta\tau} = \frac{1}{\Delta\tau^2}(2w_{\tau+\Delta\tau} - 5w_\tau + 4w_{\tau-\Delta\tau} - w_{\tau-2\Delta\tau}) \tag{18}$$

where

https://doi.org/10.1017/jmech.2014.65 Published online by Cambridge University Press

$\tau + \Delta\tau \rightarrow$ Current time step;

$\tau \rightarrow$ time step immediately preceding the current step $\tau + \Delta\tau$;

$\tau - \Delta\tau \rightarrow$ time step immediately prior to the step τ;

$\tau - 2\Delta\tau \rightarrow$ time step immediately prior to the step $\tau - \Delta\tau$;

$\Delta\tau \rightarrow$ time interval between consecutive time steps.

Since w_τ, $w_{\tau-\Delta\tau}$ and $w_{\tau-2\Delta\tau}$ are known, one can calculate $w_{\tau+\Delta\tau}$ through a system of the form:

$$Ax_{\tau+\Delta\tau} = y_{\tau+\Delta\tau} \tag{19}$$

where $x_{\tau+\Delta\tau}$ is the vector of unknown variables and $y_{\tau+\Delta\tau}$ is the vector of known variables, and that its elements are calculated from the values of w time steps earlier and boundary conditions in time $\tau + \Delta\tau$.

Since the system (19) is solved, the vector $w_{\tau+\Delta\tau}$ is known and the solution can then be found for the next time step.

7. NUMERICAL RESULTS

Some results obtained with the routines implemented are presented below. These results are compared with results obtained by finite element method and meshless methods Petrov-Galerkin (meshless Petrov Galerkin method, MLPG) proposed by Sladek *et al*. [29].

7.1 Applying this RIM for Transient Analysis in Orthotropic Plate

In this section, numerical results for moments are presented for plates under time dependent loads. The values obtained at one point of the plate are compared with results available in literature

7.1.1 Square plate simply supported on all four sides under uniformly distributed load

Consider a plate supported (Fig. 2) charged at time $\tau_o = 0$ s by a charge $q = 2{,}07 \times 1^{06}$ N/m^2 type step (Fig. 3). The plate is orthotropic and has the following properties and dimensions: $E_2 = 6895$MPa, $E_1 = 2E_2$, $G_{12} = 2651.9$MPa, $v_{12} = 0,3$, $\rho = 7166$kg/m^3, $a = 254$mm and thickness $h = 12,7$mm. This problem is equivalent to problem proposed by Sladek *et al*. (2007) that was analyzed using MPLG. The static bending moment at the center of the plate is given by $m_x^{state} = 9{,}54 \times 10^3$Nm / m for factor standardization of time $t_0 = a^2(\sqrt{\rho h / D_{22}})/4$.

7.1.1.1 Sensitivity to the Number of Internal Points

The plate was discretized using 12 quadratic discontinuous boundary elements of the same length of time steps $\Delta\tau = 3{,}9447 \times 10^{-5}$s. The problem was analyzed using 1, 9 and 25 internal points uniformly distributed. Figure 4 shows the bending moment at the center of the plate as a function of time.

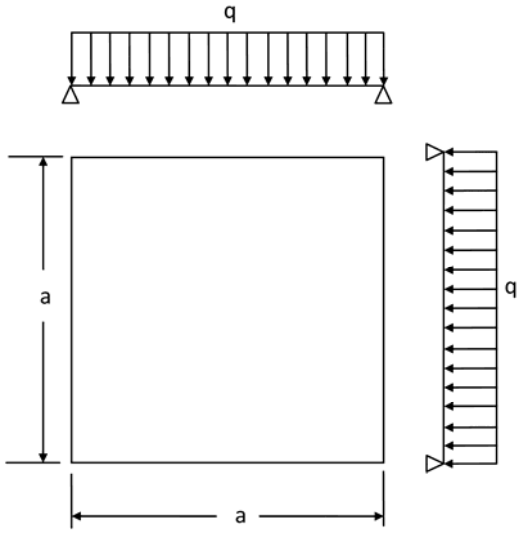


Fig. 2 Supported orthotropic square plate.

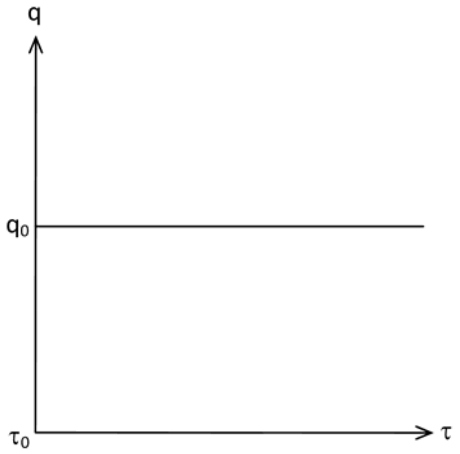


Fig. 3 Loading type step function.

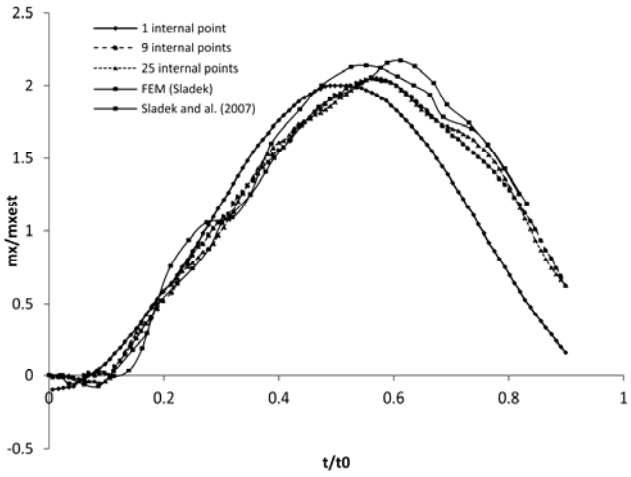


Fig. 4 Mesh with internal points in the plate.

It can be observed that the uses of internal points are necessary to achieve greater accuracy of results. In this case, the result obtained with 25 internal points was closer to the solution of finite element and MLPG that results with 1 and 9 internal points. However, results

https://doi.org/10.1017/jmech.2014.65 Published online by Cambridge University Press

at 9 and 25 points inside are very similar, which indicates a convergence of results. The results showed an internal point excessively smooth away the other results. That is, the number of internal points was insufficient for adequate modeling of this problem.

7.1.1.2 Sensitivity to the Number of Elements

The plate was discretized using nine internal points and time step $\Delta\tau = 3{,}9447 \times 10^{-5}$s. The problem was analyzed using 8, 12 and 16 quadratic discontinuous boundary elements of equal length. Figure 5 shows the bending moment at the center of the plate as a function of time.

As noted, the curves are presented in juxtaposition, indicating that only two elements per side is enough for adequate modeling of this problem.

7.1.1.3 Sensitivity to Time Step

The plate was discretized using nine internal points and 12 quadratic discontinuous boundary elements of equal length. The problem was analyzed using time steps equal to $\Delta\tau = 1{,}3149 \times 10^{-4}$s, $\Delta\tau = 3{,}9447 \times 10^{-5}$ s and $\Delta\tau = 1{,}9723 \times 10^{-5}$s. Figure 6 shows the bending moment at the center of the plate as function of time.

In this case, one can observe that there was little variation of results when the time step $\Delta\tau = 1{,}9723 \times 10^{-5}$s it used, however, for the time step $\Delta\tau = 1{,}3149 \times 10^{-4}$s result was so much smoother. This indicates that excessively large time steps tend to soothe the result, there is an optimum size at which time steps vary slightly lower results

7.1.1.4 Behavior of the Moment in a Longer Time Interval

The plate was discretized using nine internal points and time step $\Delta\tau = 3.9447 \times 10^{-5}$s. The problem was analyzed using 12 quadratic discontinuous boundary elements of equal length. Figure 7 shows the bending moment at the center of the plate as a function of time.

Observe that the curve had a slight dampening of peaks, which can be assigned to the numerical damping of the Houbolt method. However, you need a closer look and a greater number of issues to better understand the characteristics of the Houbolt method. For purposes of this work, the result was quite satisfying.

Following the same procedure done for the moment, we carried out calculations of the displacement of the central board for the same period of time. Figure 8 shows the displacement of the center of the plate as a function of time.

According to Figure 8, it was observed that the shift showed a good performance over the time interval, varying little in shape and amplitude of cycles.

7.1.2 Square Plate Clamped on All Four Sides Under Uniformly Distributed Load

Consider a clamped plate (Fig. 9) charged at time $\tau_o = 0$ s by a charge $q = 2{,}07 \times 1^{06}$ N/m^2 type step (Fig. 3). The plate has the same properties and dimensions as section 1. The only difference is the boundary condition. The static bending moment at the center of the plate is given by $m_x^{state} = 4,\ 06 \times 10^3$Nm / m and the normalization factor for time $t_0 = a^2(\sqrt{\rho h / D_{22}})/4$.

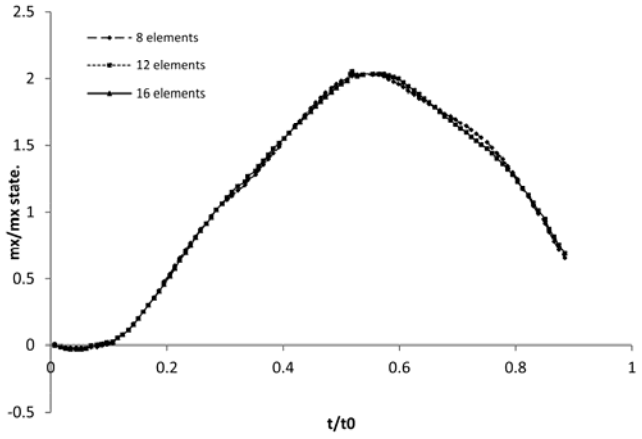


Fig. 5 Bending moment of the central plate as a function of time subject to variation of number of elements.

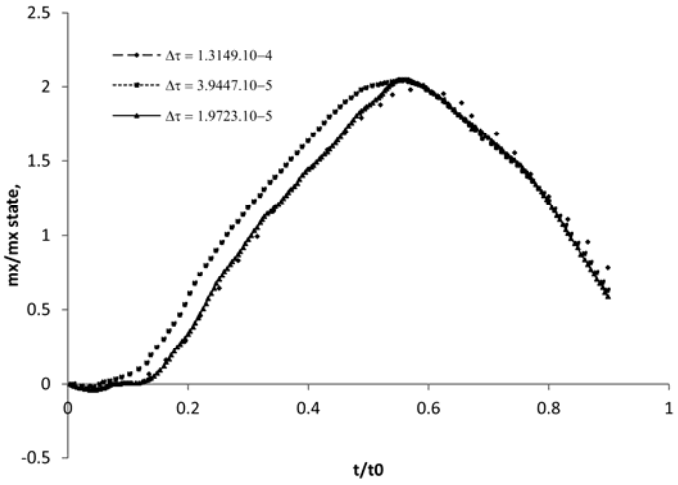


Fig. 6 Bending moment at the central plate subject to the variations of time step.

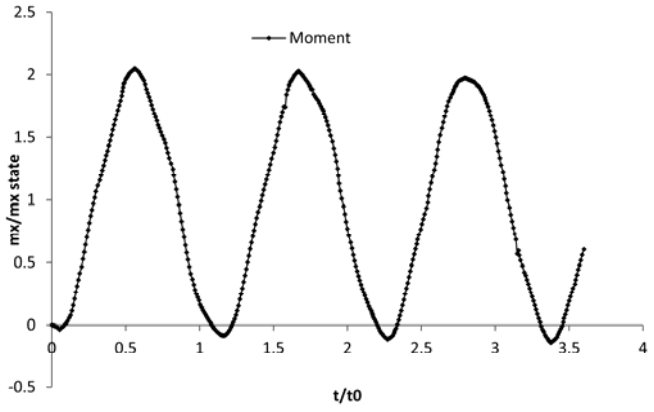


Fig. 7 Bending moment at the center of the plate.

https://doi.org/10.1017/jmech.2014.65 Published online by Cambridge University Press

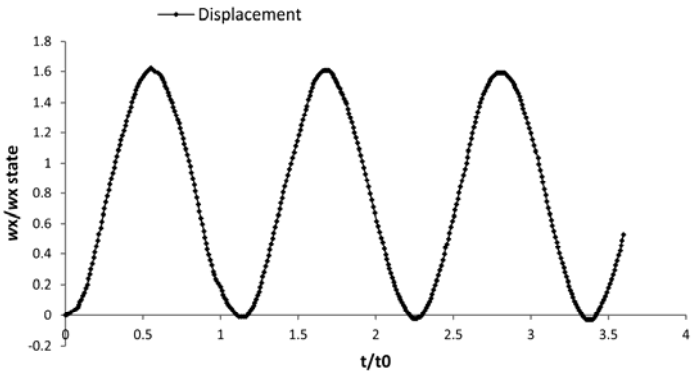


Fig. 8 Vertical displacement of the central plate.

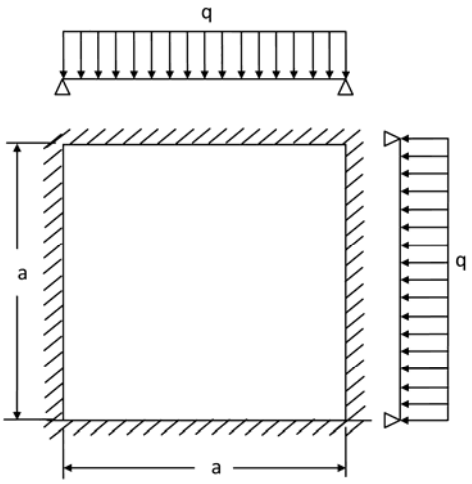


Fig. 9 Clamped orthotropic square plate.

7.1.2.1 Sensitivity to the Number of Internal Points

The plate was discretized using 12 quadratic discontinuous boundary elements of the same length of time steps $\Delta\tau = 2{,}1915 \times 10^{-5}$s. The problem was analyzed using 1, 9 and 25 internal points uniformly distributed. Figure 11 shows the bending moment at the center of the plate as a function of time. Moreover, this figure are shown the results using the finite element MLPG and presented by Sladek *et al*. [29].

It may be noted that internal points are necessary to achieve greater accuracy of results, as shown in Fig. 10. With only one internal point there is a significant difference in relation to the other results. The result with 25 internal points proved to be closest of the solutions obtained by Sladek *et al*. [29]. The result with 9 points inside was a good concordance with the results of the literature.

7.1.2.2 Sensitivity to the Number of Elements

The plate was discretized using nine internal points and time step $\Delta\tau = 2{,}1915 \times 10^{-5}$s. The problem was analyzed using 8, 12 and 16 quadratic discontinuous boundary elements of equal length. Figure 11 shows the bending moment in the center of the plate as a function of time.

It can be seen in Fig. 11 that the discretization of the contour of the plate had little effect on the results, just as in the case of the plate supported analyzed previously.

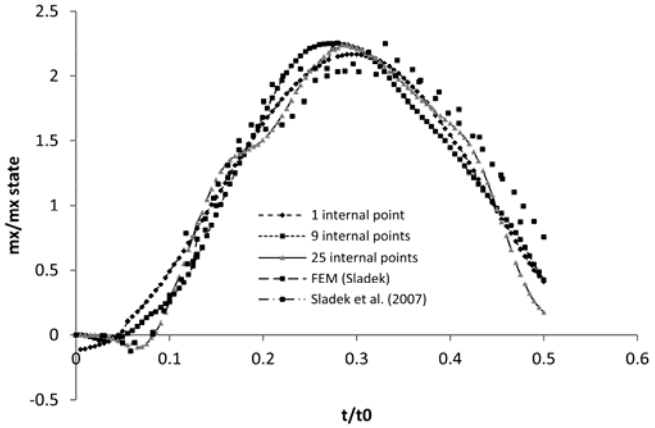


Fig. 10 Bending moment at the center of the plate as a function of time, varying the number of internal points.

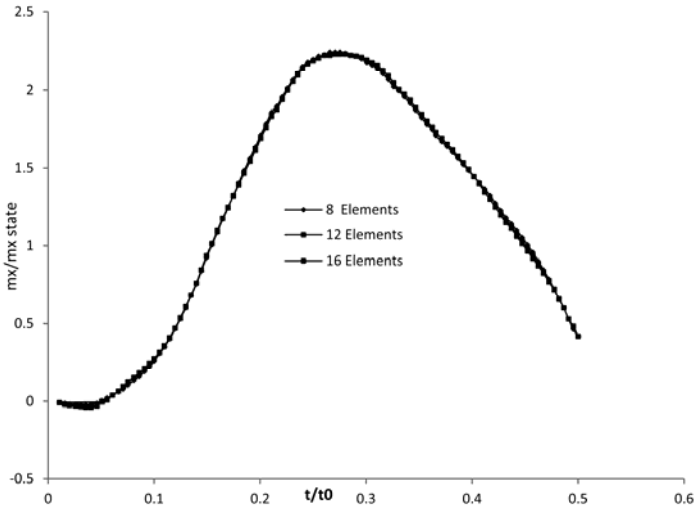


Fig. 11 Bending moment in the center of the plate as a function of time, varying the number of elements.

7.1.2.3 Sensitivity to Time Step

The plate was discretized using internal points 9 and 12 quadratic discontinuous boundary elements of equal length. The problem was analyzed using time steps equal to $\Delta\tau = 7{,}3049 \times 10^{-5}$s, $\Delta\tau = 2{,}1915 \times 10^{-5}$ and $\Delta\tau = 1{,}0957 \times 10^{-5}$s. Figure 12 shows the bending moment in the plate as a function of time.

As seen in Fig. 12, there was little variation in results when we used the time step $\Delta\tau = 7{,}3049 \times 10^{-5}$ and $\Delta\tau = 2{,}1915 \times 10^{-5}$s. However, for the time step $\Delta\tau = 1{,}0957 \times 10^{-5}$s, the result was very smooth, as noted in the previous example.

7.1.3 Plate Clamped-Free Under Uniformly Distributed Load

Consider a plate clamped-free (Fig. 13) charged at time $\tau 0 = 0$s by a load step type $q = 2{,}07 \times 10^{6}$N/m^2. The plate has considered the same properties and dimensions of Section 1. The plate was discretized using 20 quadratic discontinuous boundary elements of

https://doi.org/10.1017/jmech.2014.65 Published online by Cambridge University Press

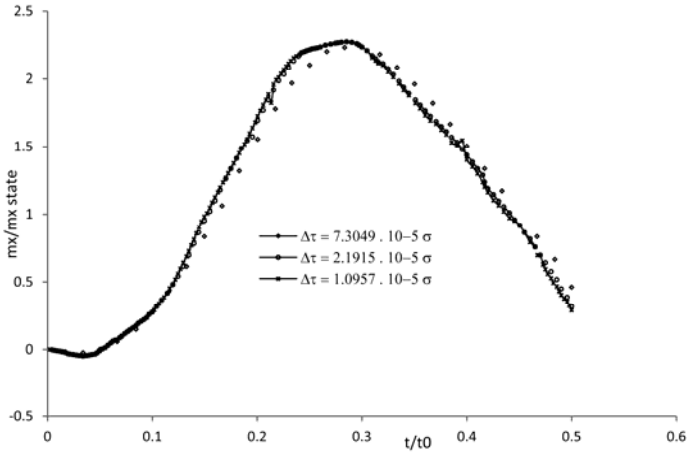


Fig. 12 Bending moment in the central plate subject to variation of time step.

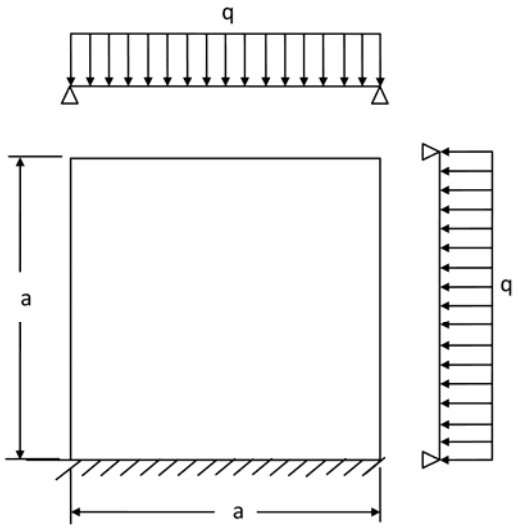


Fig. 13 Orthotropic square plate clamped on one side and free on 3 sides.

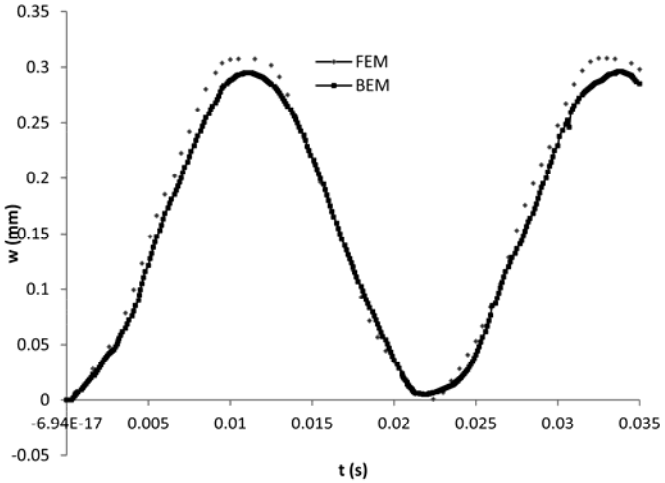


Fig. 14 Vertical displacement at the center of the plate over time.

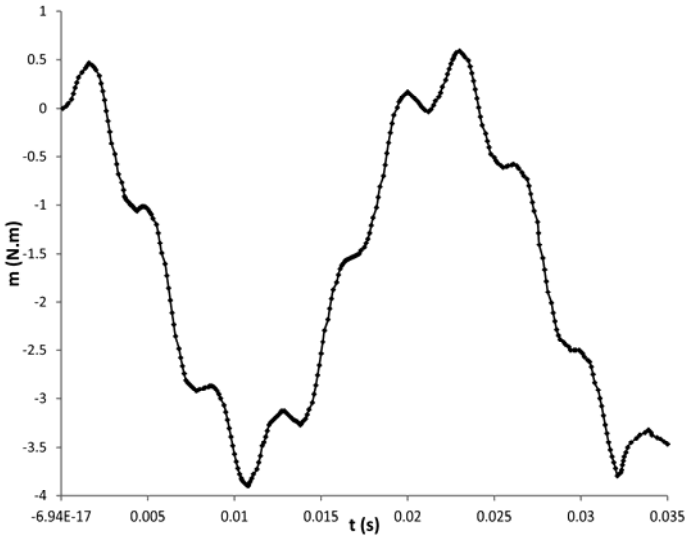


Fig. 15 Bending moment in the center of the plate over time.

equal length, time step is $\Delta\tau = 1,1667 \times 10^{-4}$ and 25 uniformly distributed internal points. Figure 14 shows the vertical displacement of the center of the plate as a function of time.

It can be seen in Fig. 14 that the results were near the finite element solution. Figure 15 shows the bending moment in the center of the plate as a function of time. It can be seen that the results remained stable throughout the analyzed interval.

8. CONCLUSIONS

This paper presented a formulation of the boundary element method for the calculation of moments, tensions and failure criteria on internal points in thin plates of composite materials. The formulation of the boundary element method for analyzing elastodynamics problems in anisotropic materials was obtained using the fundamental solutions elastostatic and considering the terms of inertia and body forces. We used quadratic discontinuous boundary elements. The domain integrals from terms of inertia were transformed into boundary integrals using the radial integration method.

The radial basis function of thin plates spline is used as an approximation function in the radial integration method augmented by polynomials, as reported in literature, presents a good performance in various formulations.

The formulation was applied to various numerical problems and showed good agreement with results available in the literature. Analysis of sensitivity to the number of internal points, number of elements and the time step size were made.

The method was sensitive to the number of internal points, requiring, in all problems a minimum number of internal points from which the response shows good agreement with literature results. When few internal points are used, the results tend to be softer.

There was little sensitivity as the number of boundary element mesh, obtaining good agreement with the literature even for very coarse meshes.

https://doi.org/10.1017/jmech.2014.65 Published online by Cambridge University Press

The method was sensitive to the size of the time step. Large time steps tend to soften the results, although still remaining with a good agreement with literature results.

Overall, the developed formulation performed well in modeling dynamic problems of thin anisotropic plates, constituting itself as an alternative to the analysis of structures of composite laminates subjected to transient loading.

ACKNOWLEDGEMENTS

The authors would like to acknowledge the "Ministry of Higher Education and Scientific Research" Project CNEPRU J0301920120029, for the fanical support of this work.

REFERENCES

1. Lakshminarayana, H. V. and Murthy, S. S. A., "Shear-Flexible Triangular Finite Element Model for Laminated Composite Plates," *International Journal for Numerical Methods in Engineering*, **20**, pp. 591–623 (1984).
2. Luo, R. K., Green, E. R. and Morrison, C. J., "Impact Damage Analysis of Composite Plates," *International Journal of Impact Engineering*, **22**, pp. 435–447 (1999).
3. Zhao, G. P. and Cho, C. D., "Damage Initiation and Propagation in Composite Shells Subjected to Impact," *Composite Structures*, **78**, pp. 91–100 (2007).
4. Ganapathy, S. and Rao, K. P., "Failure Analysis of Laminated Composite Cylindrical/Spherical Shell Panels Subjected to Low-Velocity Impact," *Computers and Structures*, **68**, pp. 627–641 (1998).
5. Li, C. F., Hu, N., Yin, Y. J., *et al*., "Low-Velocity Impact-Induced Damage of Continuous Fiber-Reinforced Composite Laminates. Part I: An Fem Numerical Model," *Composites Part A-Applied Science and Manufacturing*, **33**, pp. 1055–1062 (2002).
6. Li, C. F., Hu, N., Cheng, J. G., *et al*., "Low-Velocity Impact-Induced Damage of Continuous Fiber-Reinforced Composite Laminates. Part II: Verification and Numerical Investigation," *Composites Part A: Applied Science and Manufacturing*, **33**, pp. 1063–1072 (2002).
7. Shi, G. and Bezine, G., "Buckling Analysis of Orthotropic Plates by Boundary Element Method," *Mechanics Research Communications*, **26**, pp. 1351–1370 (1990).
8. Wu, B. C. and Altiero, N. J., "A New Numerical Method for the Analysis of Anisotropic Thin Plate Bending Problems," *Computer Methods in Applied Mechanics and Engineering*, **25**, pp. 343–353 (1981).
9. Rajamohan, C. and Raamachandran, J., "Bending of Anisotropic Plates by Charge Simulation Method," *Advances in Engineering Software*, **30**, pp. 369–373 (1999).
10. Paiva, W. P., Sollero, P. and Albuquerque, E. L., "Treatment of Hypersingularities in Boundary Element Anisotropic Plate Bending Problems," *Latin American Journal of Solids and Structures*, **1**, pp. 49–73 (2003).
11. Wang, J. and Schweizerhof, K., "Fundamental Solutions and Boundary Integral Equations of Moderately Thick Symmetrically Laminated Anisotropic Plates," *Communications in Numerical Methods in Engineering*, **12**, pp. 383–394 (1996).
12. Wang, J. and Schweizerhof, K., "Free Vibration of Laminated Anisotropic Shallow Shells Including Transverse Shear Deformation by the Boundary-Domain Element Method," *Computers and Structures*, **62**, pp. 151–156 (1997).
13. Wang, J. and Schweizerhof, K., "The Fundamental Solution of Moderately Thick Laminated Anisotropic Shallow Shells," *International Journal of Engineering Science*, **33**, pp. 995–1004 (1995).
14. Venturini, W. S., "A Study of Boundary Element Method and Its Application on Engineering Problems," Ph.D. Dissertation, Sao Carlos School of Engineering, University of Sao Paulo, Brazil (1988) (in Portuguese).
15. Gao, X., "The Radial Integration Method for Evaluation of Domain Integrals with Boundary Only Discretization," *Engineering Analysis with Boundary Elements*, **26**, pp. 905–916 (2002).
16. Albuquerque, E. L. *et al*., "Boundary Element Analysis of Anisotropic Kirchhoff Plates," *International Journal of Solids and Structures*, **43**, pp. 4029–4046 (2006).
17. Tsai, S. W. and Wu, E. M., "A General Theory of Strength Test for Anisotropic Materials," *Journal of Composite Materials*, **5**, pp. 58–80 (1971).
18. Hill, R., "A Theory of the Yelding and Plastic Flow of Anisotropic Metals," *Proceedings of the Royal Socety*, **193**, pp. 281–297 (1950).
19. Tsai, S. W., *Strength Theories of Filamentary Structures, in Fundamental Aspects of Fiber Reinforced Plastic Composites*, R.T. Schwartz and H.T. Schwartz Eds., Wiley Interscience, New York, US, pp. 3–11 (1968).
20. Lekhnitskii, S. G., *Anisotropic Plates*, Gordon and Breach, New York, US (1968).
21. Shi, G. and Bezine, G. A., "General Boundary Integral Formulation for the Anisotropic Plate Bending Problems," *Journal of Composite Materials*, **22**, pp. 694–716 (1988).
22. Paiva, J. B., "Boundary Element Formulation for Plate Bending and its Aplication in Engineering," Ph.D. Dissertation, Sao Carlos School of Engineering, University of Sao Paulo, Brazil (1987) [Text in Portuguese].
23. Albuquerque, E. L. and Aliabadi, M. H., "A Boundary Element Analysis of Symmetric Laminated Composite Shallow Shells," *Computer Methods in Applied Mechanics and Engineering*, **199**, pp. 2663–2668 (2010).
24. Houbolt, J. C., "A Reccurrence Matrix Solution for

https://doi.org/10.1017/jmech.2014.65 Published online by Cambridge University Press

the Dynamic Response of Elastic Aircraft," *Journal of Aeronautical and Science*, **17**, pp. 540–550 (1950).
25. Loeffler, C. F. and Mansur, W. J., *Analysis of Time Integration Schemes for Boundary Element Applications to Transient Wave Propagation Problems, in Boundary Element Techniques: Applications in Stress Analysis and Heat Transfer*, C. A. Brebbia and W. S. Venturini Eds., Computational Mechanics Publications, Southampton, Boston, US, pp. 105–122 (1987).
26. Albuquerque, E. L., Sollero P. and Aliabadi, M. H., "The Boundary Element Method Applied to Time Dependent Problems in Anisotropic Materials," *International Journal of Solids and Structures*, **39**, pp. 1405–22 (2002).
27. Fedelinsk, P., Aliabadi, M. H. and Rooke, D. P., "Boundary Element Formulations for the Dynamic Analysis of Cracked Structures," *Engineering Analysis with Boundary Elements*, **17**, pp. 45–56 (1996).
28. Chirino, F., Gallego, R. and Saez, A., *et al*., "A Comparative Study of Three Boundary Element Approaches to Transient Dynamic Crack Problems," *Engineering Analysis with Boundary Elements*, **13**, pp. 11–19 (1994).
29. Sladek, J., *et al*., "Local Boundary Integral Equations for Orthotropic Shallow Shells," *International Journal of Solids and Structures*, **44**, pp. 2285–2303 (2007).

(Manuscript received October 16, 2012,
accepted for publication June 10, 2014.)

https://doi.org/10.1017/jmech.2014.65 Published online by Cambridge University Press